ELSEVIER

Journal of Nuclear Materials 255 (1998) 214–221

journal of nuclear materials

Chemical erosion of CKC TiB_2-doped graphite

J.W. Davis *, A.A. Haasz

Fusion Research Group, University of Toronto, Institute for Aerospace Studies, 4925 Dufferin St., Toronto, Ontario, Canada M3H 5T6

Received 26 September 1997; accepted 23 January 1998

Abstract

The chemical erosion of graphites doped with TiB_2 has been measured for H^+ energies 30 to 1000 eV and temperatures 300 to 1100 K. The erosion yield of an undoped material, manufactured by the same process, was found to be almost identical to that of HPG99 pyrolytic graphite, while materials containing 10% and 20% TiB_2 show reduced yields. For ion energies $\gtrsim$ 300 eV and temperatures $\gtrsim$ 700 K, the erosion yield was reduced by a factor of 4 to 10 for the doped materials. For lower ion energies and temperatures, the effect of the dopants was less pronounced. For the lowest ion energies, the reduction in erosion yield was comparable to the reduction in carbon content, implying that the presence of the dopants played no role in the erosion mechanism.

1. Introduction

Doped graphites or C/C composites are viewed as an alternative to pure carbon for some of the plasma-facing components in next-generation fusion devices. Reductions in chemical erosion are the primary motivation for this choice. In a previous publication, we have reported on the reduction in erosion yield achieved through the doping of carbon with various elements: B, Ti, Si, Ni and W [1,2]. From these studies, we have determined that boron is the most effective at reducing chemical erosion [1], while titanium was the most effective at suppressing radiation-enhanced sublimation (RES) [2]. In the present series of experiments, we have extended our work to include carbon materials doped with both B and Ti, introduced in the form of TiB_2 powder. All of these doped graphites have been produced specifically for potential fusion use by Ceramics Kingston Ceramique Inc. in Canada. The results in this report are part of a four-component study, which looks at various aspects of the materials from a fusion plasma-facing material perspective. Measurements of thermal conductivity have already been performed [3], while measurements of high temperature erosion (RES) and hydrogen retention characteristics are in progress. Here we present chemical erosion measurements.

In addition to the study by Chen et al. [1], several other investigations have been performed on the chemical erosion of doped graphites due to H^+/D^+ bombardment, e.g., Refs. [4–14]. More than two decades ago, Busharov et al. [4], found the erosion of a C + SiC material, and USB15 to be $\sim$ 20 times lower than pyrolytic graphite at 873 K. In the mid-eighties, Roth [5] presented results which indicated significant yield reductions for graphites containing 0.5% B and 4% SiC when bombarded by 2 keV D^+ or H^+ ions, as compared to pyrolytic graphite. Since that time, there has been continued strong interest in doped graphites for fusion applications. It has never been clear, however, that doped graphites will have reduced erosion yields as compared to pure graphite in the ion energy and temperature range of interest for magnetic fusion. Furthermore, it is recognized that the manner in which the dopants are introduced into the graphite may also be of critical importance.

2. Experimental

All experiments were performed in our UHV accelerator facility. H_3^+ ions were produced by a low-energy,

* Corresponding author.

0022-3115/98/$19.00
PII: S0022-3115(98)00024-5

high-flux, mass-analyzed ion accelerator, and the ion beam was at normal incidence to the specimen surface. A schematic of the experimental facility is shown in Fig. 1. Measurements were made at 4 ion energies: 3 keV H_3^+ (1 keV/H^+), 900 eV H_3^+ (300 eV/H^+), 300 eV H_3^+ (100 eV/H^+) and 90 eV H_3^+ (30 eV/H^+). At the two highest energies, the specimen was biased at +30 V in order to suppress secondary electrons, while for the two lower energies, the specimen was biased at +500 V (i.e., 800 and 590 eV beams, respectively) in order to reduce the beam energy, while maintaining a fairly large beam current (7–20 μA). Biasing the specimen to +500 V will naturally introduce some error in the beam current measurements, however, measurements made of beam current while increasing the specimen bias from +30 to +500 V indicate that this error is on the order of 5–10%. Other measurements have indicated the neutral content of the beam to be $< 0.3\%$ (upper limit) at the lowest flux densities [J.W. Davis, unpublished results, 1995], and thus synergistic erosion enhancement should not significantly affect the measurements. The beam has a Gaussian-like spatial profile, limited by a 3 mm diameter aperture. Beam spots on the specimen were approximately 20 mm^2 for 300–3000 eV H_3^+ beams, and ~ 30 mm^2 for the 90 eV H_3^+ beam.

The volatile molecular products of the chemical erosion process were measured in the residual gas by a quadrupole mass spectrometer (QMS). The QMS was calibrated in situ with calibrated leaks of CH_4, C_2H_4, and C_3H_6. The sensitivity to other hydrocarbons, C_2H_2, C_2H_6 and C_3H_8, was estimated based on previous measurements of cracking patterns and relative sensitivities [15]. Matrix algebra, using the M/e signals at 15, 26, 27, 29, 30 and 41, was used to deconvolute the observed signals and evaluate the erosion yields for the six hydrocarbons listed above. Very small signals at M/e = 29, 30 and 41 may lead to greater scatter in the total chemical erosion yield data than in the data for methane only.

Since the RGA does not discriminate against background QMS signals due to ions reflecting off the specimen and interacting with carbon on the vacuum system walls [16,17], or caused by beam line effects, corrections for these effects need to be made. The correction usually does not have a large effect on peak erosion yields; however, at low and high temperatures, especially at low energy, the correction can be quite significant. After a specimen has been desorbed of hydrogen, in this case by heating to 1100 K, measurements have shown that essentially all of the non-reflected hydrogen is trapped in the graphite until near-saturation occurs [18–20]. Thus, there will be no hydrocarbons released from the specimen immediately upon turning on the beam. Experimentally, however, there is always a prompt rise in some of the hydrocarbon signals when the beam is turned on, even after desorption. This prompt rise is attributed to a wall signal and is subtracted from the measurements. The correction is assumed to be temperature independent, however, it will depend on wall conditioning and the H reflection coefficient. This correction leads to the large error bars observed for measurements at low and high temperatures.

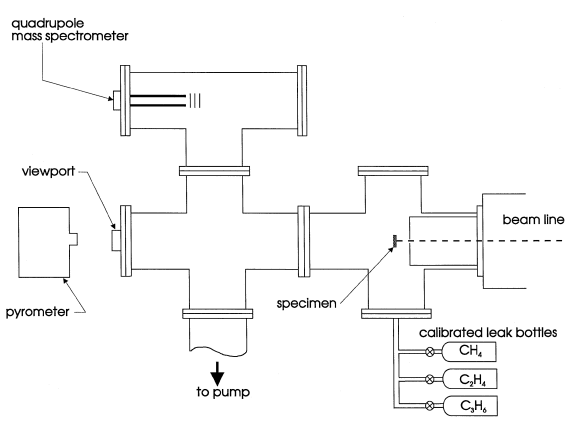

Fig. 1. Schematic of the experimental setup.

Ion energies were chosen in order of highest to lowest. In this way, long transients associated with the evolution of the surface structure were minimized. Before changing ion energies, specimens were annealed at 1100 K for 30 min, followed by a long fluence ($\gtrsim 3 \times 10^{22}$ H^+/m^2) exposure at the new ion energy. The upper temperature limit was due to the fragile nature of the doped materials when cut in thin strips.

2.1. Doped graphite materials

Material blocks containing 0, 10 and 20% TiB_2 were fabricated by Ceramics Kingston Ceramique (CKC) from finely ground pyrolytic graphite (μm-size) mixed with μm-size TiB_2 powder and an organic binder. Specimen blocks were prepared with a final heating stage at ~ 2270 K. The TiB_2 concentrations are nominal values provided by the manufacturer based on the molecular concentration of TiB_2 (N_{TiB_2}) and the atomic concentration of C (N_C); ie., $N_{TiB_2}/(N_{TiB_2} + N_C) \sim 0.1$ or 0.2. This corresponds to 8.3 at.% Ti, 16.7 at.% B and 75 at.% C for the nominal 10% TiB_2 material, and 13 at.% Ti, 27 at.% B and 60 at.% C for the nominal 20% TiB_2 material. In accordance with our previous papers [1,2], these materials are designated CKC-Ti8/B17 and CKC-Ti13/B27; the undoped reference material is designated CKC-Ref. Test specimens were cut in strips of approximate dimensions $50 \times 10 \times 0.4$ mm^3 using a diamond grinding wheel. Because of the anisotropy observed for these materials [3], specimens were cut in two orientations, which are referred to as 'edge' and 'base' orientations. 'Edge' and 'base' correspond to strips cut parallel and perpendicular to the primary axis of compression during the manufacturing process, respectively. The doped materials have a thermal conductivity decreasing from ~ 100 to 70 W/mK in the

300 to 1000 K temperature range in the 'edge' direction, which is similar to the thermal conductivity of EK98 (isotropic fine grain graphite, Ringsdorff, Germany). In the 'base' direction, the conductivity is a factor of 4–5 smaller [3].

Specimens were heated by direct current, and temperatures were measured by infrared pyrometers. In addition to the CKC specimens, new measurements were also made on HPG99 pyrolytic graphite (Union Carbide) in order to make the most direct possible comparisons.

2.2. Specimen surface analysis

The TiB_2-doped materials have been analyzed by five different techniques in order to determine various surface and bulk properties. (1) SEM photography, both regular and backscattered (compositional) mode, provides a view of the surface structure, an estimate of grain size, and a measure of how the dopants are distributed. (2) EDS, X-ray elemental analysis, provides a qualitative measure of the elemental composition of the near surface, 2–3 μm. (3) XPS provides very near surface (few monolayers) compositional and bond type information. (4) RBS provides a depth profile of Ti concentrations, and (5) NRA provides a measure of the near-surface (~ 5 μm) B concentration.

2.2.1. Scanning electron microscopy (SEM)

SEM photographs of the CKC-Ti13/B27 material are shown in Figs. 2 and 3, for the edge and base orientations, respectively. Qualitatively, the materials appear very similar to an earlier batch of CKC doped graphites [1,2]. TiB_2 particulates range in size from < 1 μm to as large as ~ 5 μm. Graphite particulates range from < 1 μm to 10 μm. There is not as noticeable a difference between the edge and base specimens as was found for the previous materials [1,2], likely due to the smaller particulate sizes. TiB_2 particulates appear to be evenly distributed, with no evidence of the clumping previously observed for the Ti dopant [2]. Beam-exposed regions show a complex surface structure typically associated with sputtering. A large increase in Ti concentration is observed on the sputtered areas; compare photos (c) and (d) in Figs. 2 and 3. It is noted that high magnification photos are sensitive to local deviations, and this leads to the observed differences between the two orientations with respect to the Ti concentrations. Lower magnification photos (not included here) show similar Ti concentrations on both orientations.

2.2.2. Energy dispersive X-ray elemental microanalysis (EDS)

This qualitative analysis confirmed that the materials were composed of carbon, boron and titanium. Analysis of

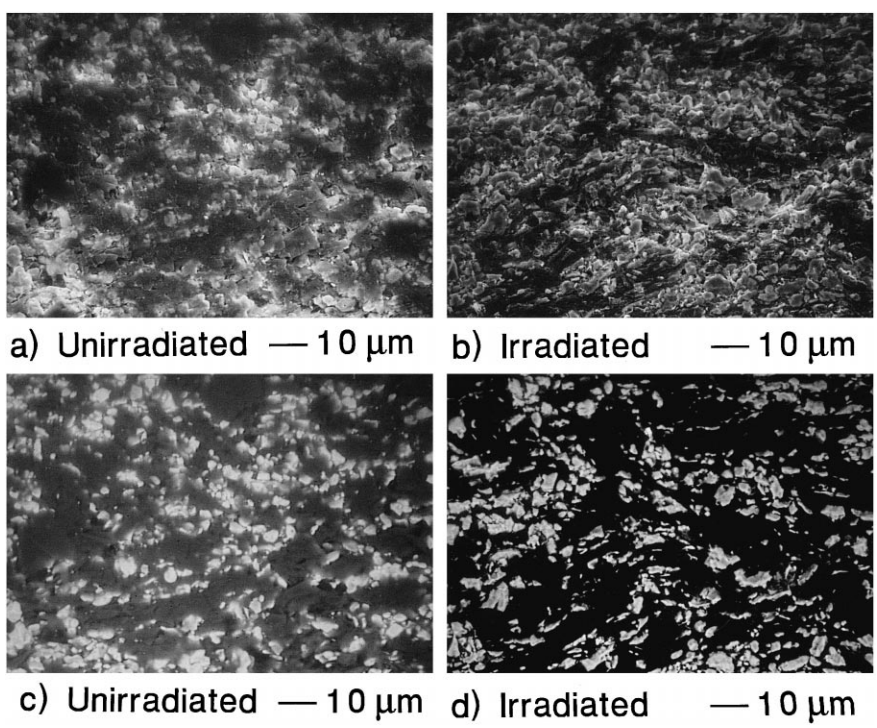

Fig. 2. SEM photographs of the CKC-Ti13/B27 edge specimen. (a) and (b) were taken in the regular, or topographical, mode; (c) and (d) in the backscattered or compositional mode, with the white areas corresponding to the TiB_2 particulates.

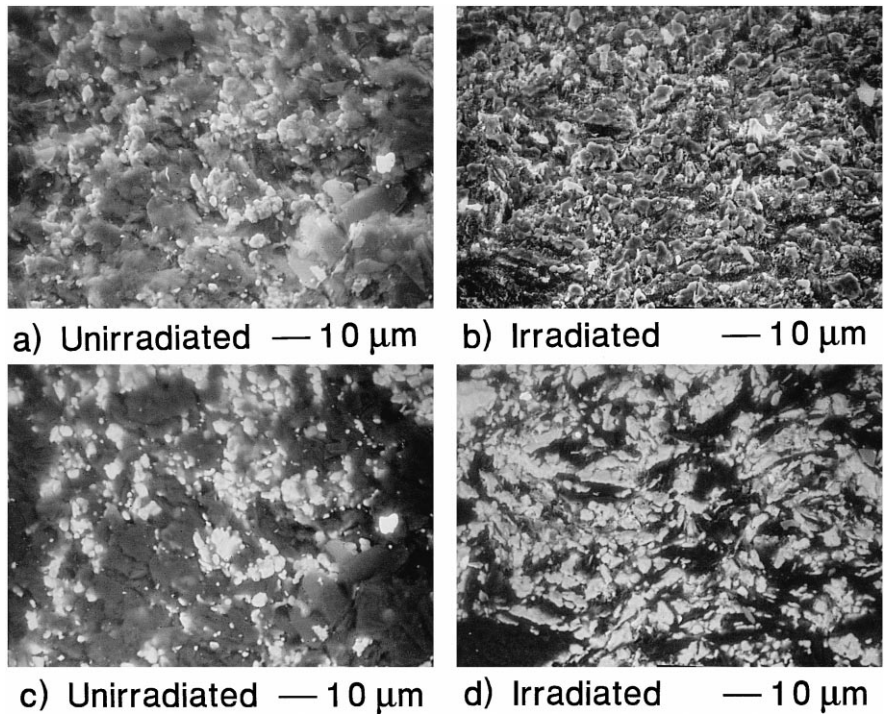

Fig. 3. SEM photographs of the CKC-Ti13/B27 base specimen. (a) and (b) were taken in the regular, or topographical, mode; (c) and (d) in the backscattered or compositional mode, with the white areas corresponding to the TiB_2 particulates.

individual grains confirmed that some were composed of B and Ti, while the remainder of the material was primarily carbon.

2.2.3. X-ray photoelectron spectroscopy (XPS)

XPS analysis was performed on the CKC-Ti13/B27 base specimen, however, the analysis is obscured by the strong interaction between the materials and air during atmospheric exposure. This led to the observation of oxide and nitride components. Bond energies attributed to TiB_2 were observed as expected.

2.2.4. Rutherford backscattering (RBS)

Depth profiles of Ti concentrations on unirradiated specimens are consistent with the nominal bulk concentrations of 8.3 at.% Ti and 14.3 at.% Ti for the nominal 10 and 20% TiB_2 materials, respectively. Near-surface concentrations of Ti are $\sim$1 at.% for the CKC-Ti8/B17 specimens and 2–3 at.% for the CKC-Ti13/B27 specimens. This is similar to surface concentrations observed in the previous set of CKC materials [2]. RBS measurements on the beam-irradiated spots show much larger surface concentrations of Ti, as was observed in both XPS and SEM analysis. On a CKC-Ti8/B17 specimen, the surface concentration was increased to $\sim$5 at.%, while on a CKC-Ti13/B27 specimen, the surface concentration was increased to $\sim$10 at.%, indicating the removal of a surface layer enriched with carbon.

2.2.5. Nuclear reaction analysis (NRA)

Integrated measurements of B concentrations were made for the CKC-Ti8/B17 and the CKC-Ti13/B27 materials. Over a depth of $\sim$5 μm, the measured B concentrations were 15 at.% (assuming an average 8 at.% Ti) and 28 at.% (assuming an average 14 at.% Ti), respectively. This is within error of the expected stoichiometry. Experimental difficulties prevented us from obtaining depth resolved B concentrations, which would have allowed us to see if enrichment or depletion of B occurs at the surface due to the ion bombardment.

3. Results and discussion

Erosion yield measurements have been made for seven specimens, and the results are presented for both the methane and total chemical erosion yields in Figs. 4–7. At 1 keV/H^+ (Fig. 4), fairly narrow erosion peaks are observed, with the maximum erosion occurring between 750 and 850 K. The doping with TiB_2 has a very similar effect to doping with B individually. In Fig. 4a, the methane yields as measured in our previous study on singly-doped graphites are compared with the present results. For the

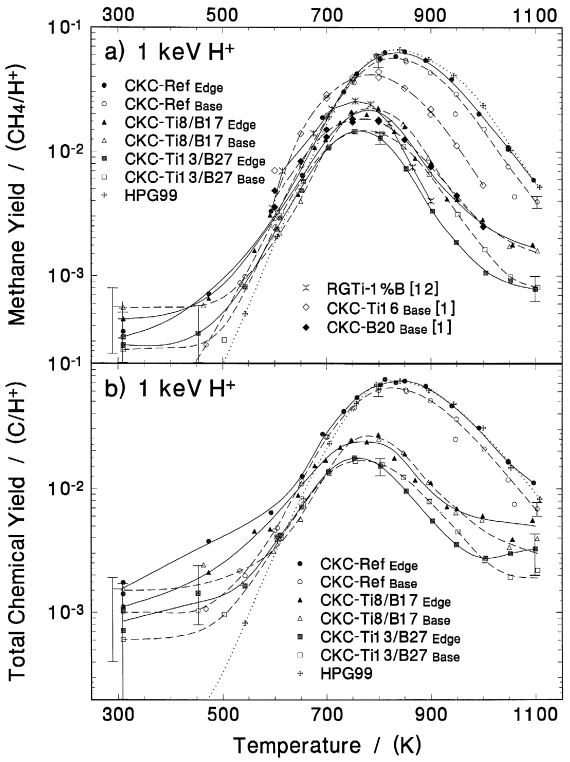

Fig. 4. (a) Methane production due to 3 keV H_3^+ (1 keV/H^+ at $\sim 5\times10^{19}$ H^+/m^2 s) bombardment of the TiB_2-doped graphites and reference specimens. (b) Total chemical erosion yield based on the sum of the erosion yields for the hydrocarbons: CH_4, C_2H_2, C_2H_4, C_2H_6, C_3H_6 and C_3H_8. Also shown for comparison in part (a) are the methane yields of the single dopant specimens previously studied [1], and results for 1 keV D^+ erosion of RGTi–1% B [12].

single-dopant materials, the largest reductions occurred for the 10 and 20 at.% B base specimens; Ti was not as effective at reducing methane production. The good agreement between the present results and the old results for B-doped graphites [1] indicates that TiB_2 is just as effective as pure B in suppressing chemical erosion. In contrast to our previous CKC materials [1], no significant differences were observed between the two orientations of the same material in the present study. Improved manufacturing techniques are a possible explanation.

At 300 eV/H^+ (Fig. 5), the erosion profiles are somewhat broader, and the temperature of the maximum erosion yield, T_m, has shifted to lower temperature. Upon reducing the H^+ energy to 100 eV (Fig. 6), a noticeable broadening and lowering of the erosion profile is observed, with a pronounced shift in the location of T_m. At 30 eV/H^+ (Fig. 7), the temperature dependence becomes even weaker, with somewhat lower T_m and Y_m. Consistent with most other results on the erosion of doped graphites [1,4–14], the effect of the dopants is more pronounced at higher temperatures and higher ion energies, >100 eV. For H^+ energies of 300 and 1000 eV, and temperatures $\gtrsim 700$ K, erosion yields are reduced by a factor of 4–10. At lower temperatures (<600 K), reductions in erosion yields are less than a factor of ~ 2 at all energies studied. At 100 eV/H^+, again yield reductions primarily occur at temperatures >700 K, but the effects are not as large, generally a factor of 3–4. At 30 eV/H^+, the scatter in the data is more pronounced due to smaller signals, and it is only possible to say that the dopants reduce the erosion yield by less than a factor of 2 over the entire temperature range. Considering that the CKC-Ti13/B27 specimens contain only 60 at.% C, this reduction at 30 eV/H^+ could be explained solely on the basis of dilution, without preferential erosion of C.

The shape of the erosion profiles is generally similar for the methane and total chemical erosion yields (comparison of parts (a) and (b) in Figs. 4–7). At 1 keV/H^+, the production of heavier hydrocarbons at T_m contributes only 20–30% to the total chemical erosion yield, while at 30 and 100 eV/H^+, they contribute more than a factor of 2, in agreement with the recent results of Mech et al. [21]

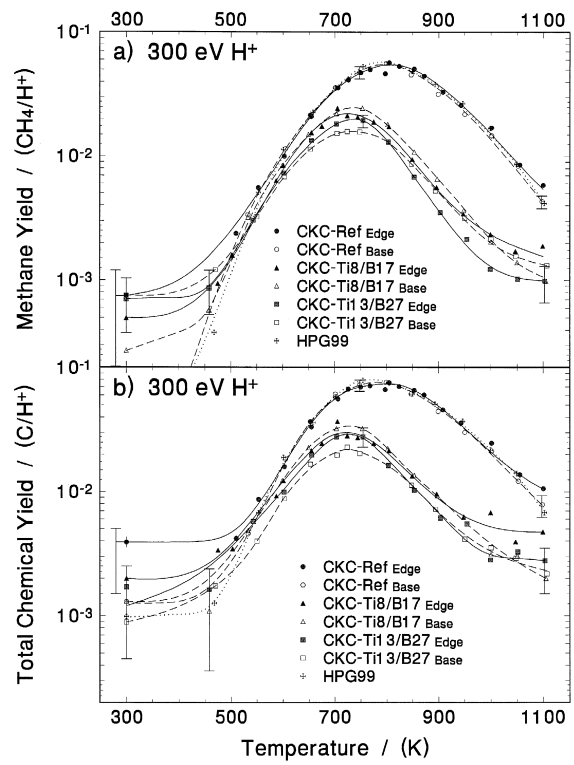

Fig. 5. (a) Methane production due to 900 eV H_3^+ (300 eV/H^+ at $\sim 2\times10^{19}$ H^+/m^2 s) bombardment of the TiB_2-doped graphites and reference specimens. (b) Total chemical erosion yield based on the sum of the erosion yields for the hydrocarbons: CH_4, C_2H_2, C_2H_4, C_2H_6, C_3H_6 and C_3H_8.

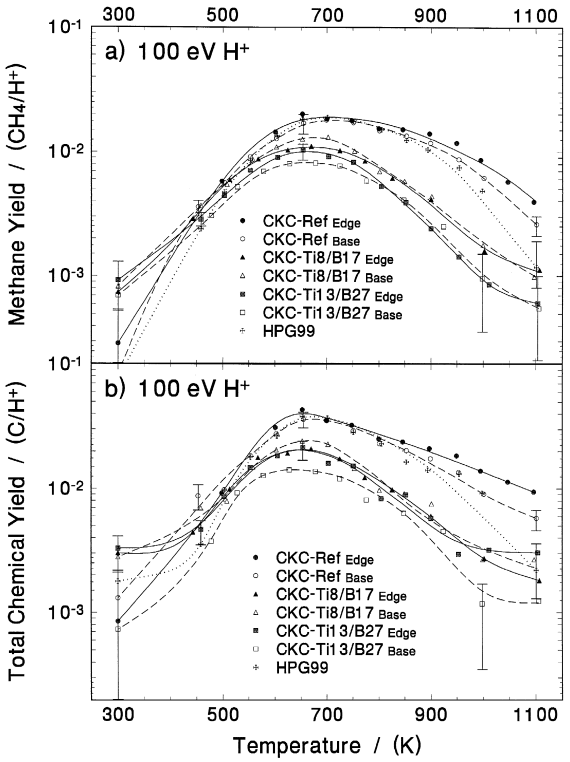

Fig. 6. (a) Methane production due to 300 eV H_3^+ (100 eV/H^+ at $\sim 1\times10^{19}$ H^+/m^2 s) bombardment of the TiB_2-doped graphites and reference specimens. (b) Total chemical erosion yield based on the sum of the erosion yields for the hydrocarbons: CH_4, C_2H_2, C_2H_4, C_2H_6, C_3H_6 and C_3H_8.

for pure graphite. Therefore, the presence of TiB_2 does not appear to have a significant effect on the ratio of methane to heavy hydrocarbon formation. We also note that the <100 eV/H^+ cases, in comparison with the 1 keV/H^+ case, differ in the temperature dependence for the production of the different hydrocarbons, leading to different shapes for the total chemical yield profiles as compared to methane. Most importantly, for <100 eV energy, the total chemical erosion yields at lower temperatures have more contribution due to heavier hydrocarbons; this effect is again similar to the pure graphite case [21].

Previous measurements of chemical erosion yields for doped graphites with relatively high ion energies, $\gtrsim 1$ keV/H^+ or D^+ [1,5,9–13] are generally in agreement with the current results. For temperatures >700–800 K, there is a large reduction in chemical erosion yield, while for temperatures $\lesssim 600$ K, dopants do not have much effect. For lower ion energies, the results are less consistent. For the case of 250 eV D^+ bombardment of B-doped GB110, GB120 and GB130 (Toyo Tanso, Japan), Hirooka et al. [7,8] found the total erosion yield (physical + chemical + RES) to be lower by a factor of 2–3 over the entire temperature range, 500–1900 K. This is markedly different from the current 300 eV H^+ results. Franconi et al. [6] found that the erosion of a SiC-impregnated graphite (Schunk-Ebe), with $\sim 33\%$ SiC, by 100 eV D^+ was reduced by a factor of 2–3 over the temperature range studied (625–1225 K), compared with an isotropic graphite. Surface analysis (AES) revealed a Si/C ratio of ~ 7, indicating that dilution could be a major cause of the yield reduction. In the latter case, the reduction is similar to our present results, however, yields were in general lower than ours.

García-Rosales and Roth [11] compared the erosion of pyrolytic graphite and USB15 and found essentially the same CD_4 yield for temperatures <600 K, at 50, 200 and 1000 eV D^+. At higher temperatures, larger reductions were observed for the USB15 specimen exposed to 50 eV D^+ ions than in our current 30 or 100 eV H^+ cases; reduced CD_4 production by an order of magnitude at 800 K were observed in Ref. [11]. In later experiments, Garcia-Rosales et al. [12] found RGTi (Ti-doped graphites, 1.7 at.% Ti) to be less effective than B-doped USB15 at reducing CD_4/D^+ yields for 1 keV D^+ bombardment.

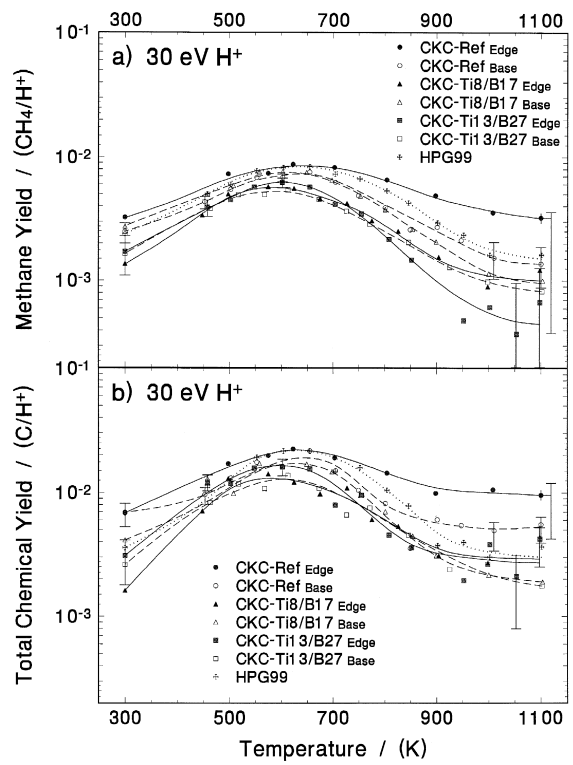

Fig. 7. (a) Methane production due to 90 eV H_3^+ (30 eV/H^+ at $\sim 5\times10^{18}$ H^+/m^2 s) bombardment of the TiB_2-doped graphites and reference specimens. (b) Total chemical erosion yield based on the sum of the erosion yields for the hydrocarbons: CH_4, C_2H_2, C_2H_4, C_2H_6, C_3H_6 and C_3H_8.

However, the factor of three reduction in yield for temperatures > 700 K is significantly larger than observed previously on a CKC 2% Ti specimen [1]. Total yields (physical + chemical) at room temperature and 50, 100 and 1000 eV D^+ were essentially the same for RGTi and pyrolytic graphite. Results for RGTi-1%B (1.7 at.% Ti and 1 at.% B) [12] were somewhat reduced compared to the RGTi yields for 1 keV D^+ bombardment. Even though the bulk dopant concentrations are much lower, the reduction in the methane yield is similar to that observed for our present TiB_2-doped materials, see Fig. 4. This indicates that the form of the dopant within the material, or the microstructure of the material may play a critical role in the erosion mechanism. Also, actual surface concentrations of the dopants during bombardment may be significantly different from the bulk values [1,2], possibly making erosion less sensitive to variations in bulk concentrations.

Recent results by Grote et al. [14], comparing a Si-doped CFC (NS 31, SEP) and an undoped CFC (Concept II, Dunlop), found the maximum total chemical erosion yield at ~ 800 K due to 30 eV H^+ was lower by a factor of 2 for the doped material, falling from 0.02 C/H^+ to 0.01 C/H^+. This is essentially identical to our present results. Below ~ 673 K, however, no difference between the erosion of the doped and undoped CFC's was observed in Ref. [14].

In addition to B, Si and Ti, chemical erosion of V-doped graphites (10, 14, 23, 29 wt.% V) has been reported by Hino et al. [13]. For 1.5 keV H^+, the total yield (physical + chemical) was reduced by only $\sim 20\%$ in strong contrast to measurements on B-doped materials [13], but similar to measurements with some Ti-doped materials [1,10].

It has been proposed that two reaction channels contribute to the formation of hydrocarbons during H^+ bombardment of graphite [22]. There is a 'high temperature' channel, which dominates for high energy (> 100 eV) impact, having a peak near 800 K; and a 'low temperature' channel, which leads to hydrocarbon formation near room temperature, that is more important during low energy (< 100 eV) bombardment. It appears that dopants have the general effect of suppressing the high temperature channel, while having only a minor influence on the low temperature channel. In more detailed modelling of the erosion chemistry [23], thermally activated reactions dominate the high temperature reaction channel, while the low temperature branch depends on the kinetic ejection of methyl groups [24]. Dopants may act to suppress the high temperature reactions through increasing hydrogen recombination [7,9], or through decreasing other chemical steps. The kinetic processes, however, are not expected to be affected by the presence of the dopants, other than through dilution of the carbon atoms [23]. There is, therefore, a general understanding of the experimental observation that dopants have little influence on the chemical erosion yield under low temperature (all energies) or low energy (all temperatures) H^+ bombardment of graphite.

4. Summary

The chemical erosion of graphite materials doped with TiB_2 has been studied for ion energies of 30 to 1000 eV/H^+, and temperatures 300 to 1100 K. The effect of the dopants is most pronounced for the higher ion energies, and for temperatures > 800 K. The results are similar to previous measurements on materials doped individually with B [1,9–11,13]. For ion energies $\lesssim 100$ eV/H^+ or D^+ (see also Refs. [6,11,12,14]), it appears that only minor reductions occur in erosion yields of doped graphites; reductions which may be comparable to the reduction observed in the C concentration at the surface, in agreement with our understanding of the two-channel erosion mechanism [23].

Acknowledgements

This work was supported by the Canadian Fusion Fuels Technology Project and the Natural Sciences and Engineering Research Council of Canada. We thank Ceramics Kingston Ceramique Inc. for supplying the TiB_2-doped graphite, and Charles Perez for preparing the specimens. Surface analysis using SEM and EDS was performed by Dr. J. Kleiman of the Integrity Testing Laboratory (Toronto, Canada) and XPS measurements were performed by the Surface Science Group at the University of Western Ontario (London, Ontario). RBS and NRA measurements were made by Dr. R. Macaulay-Newcombe at McMaster University (Hamilton, Ontario).

References

[1] A.Y.K. Chen, A.A. Haasz, J.W. Davis, J. Nucl. Mater. 227 (1995) 66.
[2] P. Franzen, A.A. Haasz, J.W. Davis, J. Nucl. Mater. 226 (1995) 15.
[3] J.W. Davis, A.A. Haasz, J. Nucl. Mater. 252 (1998) 150.
[4] N.P. Busharov, V.M. Gusev, M.I. Guseva, Yu.L. Krasulin, Yu.V. Martynenko, S.V. Mirnov, I.A. Rozina, Atomn. Energ. 42 (1977) 486.
[5] J. Roth, J. Nucl. Mater. 145–147 (1987) 87.
[6] E. Franconi, Y. Hirooka, R.W. Conn, W.K. Leung, B. Labombard, R.E. Nygren, J. Nucl. Mater. 162–164 (1989) 892.
[7] Y. Hirooka, R.W. Conn, T. Sketchley, W.K. Leung, G. Chevalier, R. Doerner, J. Elverum, D.M. Goebel, G. Gunner, M. Khandagle, B. Labombard, R. Lehmer, P. Luong, Y. Ra, L. Schmitz, G. Tynan, J. Vac. Sci. Technol. A 8 (1990) 1790.
[8] Y. Hirooka, R. Conn, R. Causey, D. Croessmann, R. Do-

erner, D. Holland, M. Khandagle, T. Matsuda, G. Smolik, T. Sogabe, J. Whitley, K. Wilson, J. Nucl. Mater. 176&177 (1990) 473.
[9] J.W. Davis, A.A. Haasz, J. Nucl. Mater. 195 (1992) 166.
[10] C. Garcia-Rosales, E. Gauthier, J. Roth, R. Schwörer, W. Eckstein, J. Nucl. Mater. 189 (1992) 1.
[11] C. García-Rosales, J. Roth, J. Nucl. Mater. 196–198 (1992) 573.
[12] C. Garcia-Rosales, J. Roth, R. Behrisch, J. Nucl. Mater. 212–215 (1994) 1211.
[13] T. Hino, K. Ishio, Y. Hirohata, T. Yamashina, T. Sogabe, M. Okada, K. Kuroda, J. Nucl. Mater. 211 (1994) 30.
[14] H. Grote, W. Bohmeyer, H.-D. Reiner, T. Fuchs, P. Kornejew, J. Steinbrink, J. Nucl. Mater. 241–243 (1997) 1152.
[15] J.W. Davis, A.A. Haasz, P.C. Stangeby, J. Nucl. Mater. 155–157 (1988) 234.
[16] A.A. Haasz, B.V. Mech, J.W. Davis, J. Nucl. Mater. 231 (1996) 170.
[17] B.V. Mech, A.A. Haasz, J.W. Davis, J. Nucl. Mater. 241–243 (1997) 1147.
[18] R. Siegele, J. Roth, B.M.U. Scherzer, S.J. Pennycook, J. Appl. Phys. 73 (1993) 2225.
[19] A.A. Haasz, J.W. Davis, J. Nucl. Mater. 209 (1994) 155.
[20] A.A. Haasz, J.W. Davis, J. Nucl. Mater. 232 (1996) 219.
[21] B.V. Mech, A.A. Haasz, J.W. Davis, Isotopic effects in hydrocarbon formation due to low-energy H^+/D^+ impact on graphite, J. Nucl. Mater., submitted.
[22] E. Vietzke, A.A. Haasz, Chemical Erosion, in: W.O. Hoffer, J. Roth (Eds.), Physical Processes of the Interaction of Fusion Plasmas with Solids, Academic Press, San Diego, 1996, p. 93.
[23] B.V. Mech, A.A. Haasz, J.W. Davis, A model for the chemical erosion of graphite due to low-energy H^+ and D^+ impact, J. Appl. Phys., submitted.
[24] J. Roth, C. Garcia-Rosales, Nucl. Fusion 36 (1996) 1647.